

Nucleation of water vapor on ions: numerical modeling

S. V. Shevkunov

St. Petersburg State Technical University, 195251 St. Petersburg, Russia

(Submitted 9 December 1993)

Zh. Eksp. Teor. Fiz. **105**, 1258–1279 (May 1994)

Heterogeneous nucleation of atmospheric water vapor on sources of strong microscopic electric fields (ions) has been modeled by means of the Monte Carlo technique using an open statistical ensemble. The intermolecular interaction is described by the ST2 potential; nonpair interactions are taken into account through the polarization of the ions and molecules. The strong nonuniform field of the ions stabilizes the nucleate of the dense phase. The stable size of the nucleate depends sensitively on external conditions (temperature and water-vapor content of the gaseous medium). The nucleate has a stable structure with an irregular spatial density profile. The main factor determining the structure of the nucleate is the strong water-ion interaction. Even in relatively dry air, essentially all ions are hydrated and carry from a few to a few dozen water molecules.

I. INTRODUCTION

Heterogeneous nucleation of water vapor on microscopic sources of strong electric fields is responsible for active effects on atmospheric processes, including artificial formation and dissipation of cloud cover. Nucleation centers may be provided by the surface of crystalline aerosols, defects in the ion crystalline lattice, and individual ions. Nucleation alters the transparency and the thermal transfer regime in the atmosphere and can act as a trigger, providing a start for the growth of unstable atmospheric processes in which enormous energies are released. Enhanced electrical charge content in the atmosphere is a side effect of industrial activity and high-energy field experiments and affects the global environment. The mobility of hydrated electrical charges affects atmospheric conductivity, atmospheric electric current, and thunderstorm activity. The electric field is the final link in a complex chain of effects of meteorological conditions on the physiological and emotional condition of human beings.

The interaction between ions and water vapor determines the electrical strength of air gaps. Practically any experiment involving ionization in a moist gaseous medium has to deal not with free ions, but with ionic complexes carrying a "coat" of several or several dozen or more water molecules. The effective radius, mobility, and dynamical stability of such complexes depends on the temperature and density of the water vapor.

These and other factors underlie the importance of the processes involved in the interaction between ions and water vapor. Such interactions must be studied at the micro-molecular level, since the dimensions of the microdroplets (clusters) that form are comparable with molecular dimensions. Because of the strong nonuniformity and the microscopic nature of the system, ordinary techniques for thermodynamic description such as the continuous-medium approximation and the classical theory of capillarity cannot be employed. Computer simulation (the Monte Carlo method and molecular dynamics) turns out to be ideal for such purposes. The techniques of numerical simulation stem from the fundamental principles of statis-

tical mechanics, and involve no uncontrolled approximations. Consequently, they belong to the class of "exact" techniques.

In the earliest work on numerical simulation of water clusters in the presence of ions¹⁻¹⁰ it was not intended to study the thermodynamic stability of a microdroplet; the size of a cluster was prescribed arbitrarily, which corresponds to the absence of material contacts with the gaseous phase and to the canonical (NVT) statistical ensemble.¹¹ In the present work the Monte Carlo method¹² is used to model the water microdroplets that form on Ag^+ and I^- ions under conditions of thermal and material contact with the gaseous phase when the temperature and vapor density are prescribed according to the typical conditions in the atmosphere at altitudes of 1–5 km. The calculations reproduce the grand canonical (μ V T) statistical ensemble. The present work initiates a series of studies of heterogeneous nucleation by numerical techniques, so the physical model and the intermolecular potential used are discussed in detail.

2. THE HAMILTONIAN OF THE SYSTEM

a) Water-water interaction

The first work on numerical simulation of water at the molecular level by the Monte Carlo method came out in 1969 (Barker and Watts¹³). The intermolecular interaction was described by a four-center pairwise Rowlinson potential cut off at a separation of 6.2 Å. Rahman and Stillinger^{14,15} proposed an effective pair interaction potential for water molecules (the ST potential), which after a number of corrections is now used in ongoing studies. The parameters of the potential were obtained by solving the inverse thermodynamic problems: by varying the intermolecular interaction they approximated the equilibrium thermodynamic properties of the liquid phase in a numerical experiment to the properties of real water (the nonpair contributions to the energy are effectively included in the pair potential). Strictly speaking, this treatment of the multiparticle contributions yields a pair pseudopotential that depends on temperature, whose use was justified in

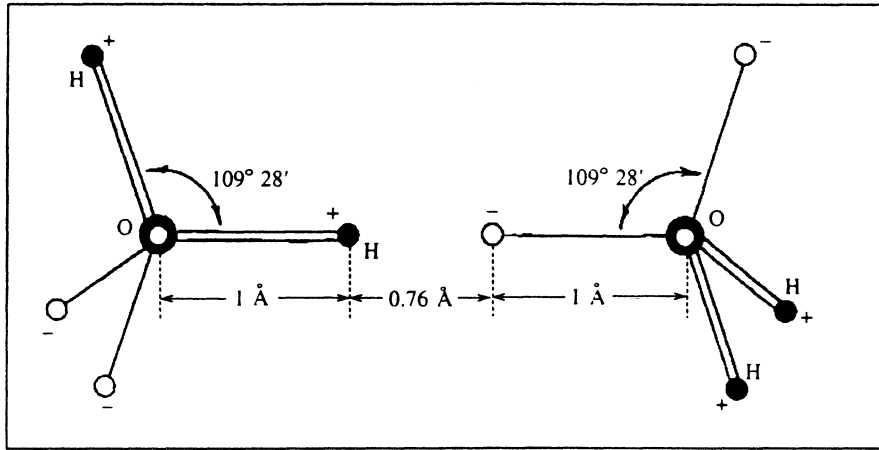


FIG. 1. The displacement of the force centers in the unmodified ST intermolecular potential. Point charges of $\pm 0.19e$ each are located at the vertices of a tetrahedron; the source of the Lennard-Jones interaction is at the geometrical center, on the oxygen atom. The configuration shown in the figure corresponds to the absolute minimum interaction energy in a molecular dimer, $U_{\min} = -0.2818$ ev.

Refs. 14 and 15 only under conditions close to those of the liquid phase. The ST potential consists of a spherically symmetric part $v_{LJ}(r_{ij})$ and an electrostatic interaction $v_{el}(\mathbf{x}_i, \mathbf{x}_j)$ between point charges displaced with respect to the geometrical center of the molecule. At small distances the electrostatic interaction is continuously reduced by some special smoothing function $s(r_{ij})$:

$$u_{\text{eff}}(\mathbf{x}_i, \mathbf{x}_j) = v_{LJ}(r_{ij}) + s(r_{ij}) \cdot v_{el}(\mathbf{x}_i, \mathbf{x}_j). \quad (1)$$

The spherically symmetric part contains the short-range exchange and dispersive interaction, and is given in the form of a Lennard-Jones potential:

$$v_{LJ}(r_{ij}) = 4\epsilon \left[\left(\frac{\sigma}{r_{ij}} \right)^{12} - \left(\frac{\sigma}{r_{ij}} \right)^6 \right] \quad (2)$$

with parameters $\epsilon = 5.01 \cdot 10^{-15}$ erg, $\sigma = 2.82$ Å. The sources of the electrostatic interaction (the four point charges) include two positive ones with $+0.19e$ and two negative ones with $-0.19e$ located at the vertices of a tetrahedron with separations of 1 Å from the Lennard-Jones force center:

$$v_{el}(\mathbf{x}_i, \mathbf{x}_j) = (0.19562e)^2 \times \sum_{\alpha_i, \alpha_j=1}^4 (-1)^{\alpha_i + \alpha_j} / d_{\alpha_i \alpha_j}(\mathbf{x}_i, \mathbf{x}_j), \quad (3)$$

where $d_{\alpha_i \alpha_j}(\mathbf{x}_i, \mathbf{x}_j)$ is the separation between the α_i and α_j charges in the i th and j th molecules. The smoothing function

$$s(r_{ij}) = \begin{cases} 0, & (0 < r_{ij} < R_L) \\ (r_{ij} - R_L)^2 (3R_U - R_L - 2r_{ij}) / (R_U - R_L)^3, & (R_L < r_{ij} < R_U) \\ 1, & (R_U < r_{ij} < \infty) \end{cases} \quad (4)$$

reduces the interaction between the point charges for $r_{ij} < R_U$ and is a reflection of the fact that the displaced charge of the electron cloud in a real H_2O molecule is distributed throughout the volume of the molecule, not concentrated at points. The original version of the ST potential had parameters $R_L = 2.0379$ Å and $R_U = 3.1877$ Å. The ST potential reaches its absolute minimum of $-4.514 \cdot 10^{-13}$ erg when the two water molecules are oriented so as to form a hydrogen bond of length $r_{ij} = 2.76$ Å.

Then the two opposite point charges $+0.19e$ and $-0.19e$ belonging to different molecules are separated by 0.76 Å (Fig. 1). The geometry of the point-charge distribution, which mimics the charge distribution in the electron clouds of an H_2O molecule, does not precisely reflect the location of the nuclei in the molecule. In particular, the charge separation of 1 Å is somewhat greater than the distance between the hydrogen and oxygen atoms in a real isolated molecule, 0.957 Å. The H-O-H angle of $109^\circ 28'$, corresponding to a regular tetrahedron, is also somewhat larger than the experimentally measured value $104^\circ 31'$. The geometrical parameters cannot be in complete agreement, if only because the ST potential models the interaction of molecules in the liquid phase, incorporating the intramolecular deformation (nonpair contributions). Stillinger and Rahman developed corrections for the ST potential,¹⁵⁻¹⁹ the improved potential received the appellation ST2. According to the authors¹³⁻²⁰ the ST potential gives rise to excessively short and narrow directed hydrogen bonds. In the ST2 potential the negative point charges which model the electrostatic part of the interaction are shifted closer to the Lennard-Jones center of the molecule, from 1 Å to 0.8 Å. This destroys the geometrical symmetry of the positive and negative charge locations. The important role of asymmetry in the location of the charges has been confirmed experimentally through the selective interaction of water molecules with charges of opposite signs. All four charges in the core of the molecule are increased by 20% to a value $q = \pm 0.2357e$, in agreement with the value of the multipole moments of a real H_2O molecule. The radius of the smoothing action of the $s(r_{ij})$ function is reduced by 2% to $R_L = 2.0160$ Å, $R_U = 3.1287$ Å, while the radius of the Lennard-Jones interaction is increased by 10% to $\sigma = 3.10$ Å, and its depth is increased by 5% to $\epsilon = 5.2605 \cdot 10^{-15}$ erg. As a result of these changes the length of the hydrogen bond in a molecular dimer has been increased by 3%, and the binding energy of a molecular pair has been reduced by 1%. The molecular dipole moment has increased from $\mu_D = 2.170D$ (ST) to $\mu_D = 2.353D$ (ST2), which is larger by 20% than the experimental value for an isolated molecule, $\mu_D^{\text{exp}} = 1.83D$. The difference in the dipole moments is related to the implicit treatment of the nonpair contributions, which are estimated to be 15% of the binding energy in a water

crystal;¹⁶ the mutual polarization of the molecules causes μ_D to increase. These modifications introduced into the ST potential have improved both the agreement of the simulated thermodynamic properties of water with experimental data and the agreement of the molecular correlation functions with experiments on x-ray scattering. In simulating water microclusters, Briant and Burton^{1,2} used the ST2 potential, but with a reduced depth $\varepsilon = 5.01 \cdot 10^{-15}$ erg for the Lennard-Jones part of the potential. The Monte Carlo method has been used to compare the equilibrium properties of water using the ST and ST2 techniques and the properties of water with the Rowlinson potential, which differs in having a greater asymmetry in the locations of the charges in the molecule.²¹ All three models displayed good reproducibility for the close molecular order.

A fundamentally different path to constructing a model intermolecular potential was taken by Abraham and Mruzik^{3,4} and also by Kistenmacher *et al.*,^{5,6} namely, quantum mechanical calculations. Popkie *et al.*⁵ calculated the interaction energy in the Hartree-Fock approximation for 216 different relative orientations of the two water molecules. The calculated energies were used to select a simple analytic expression in the form of a four-center potential. In contrast to the ST and ST2 models, the short-range repulsion was written in the form of an exponential and localized not at the center of the molecule but at the force centers of the electrostatic part of the potential. The Hartree-Fock approximation does not include quantum-mechanical correlations (exchange and Coulomb) in the electron clouds of the molecules. In Ref. 6 the contribution from the interelectron correlations to the equilibrium properties of water was evaluated. The correlations were described semiempirically. For small intermolecular separations the Wiener density-functional approximation was employed for the electron gas, while at large separations the asymptotic form $\sim r^{-6}$ (dispersion interaction) was used with the coefficients of London and Kirkwood. The correlation corrections were approximated using functions localized at the oxygen atoms. The Kirkwood correction at intermediate separations was represented in the form $c \cdot \exp(-\delta r)$ with $\delta = 0.9752 \text{ \AA}^{-1}$ and $c = 64.62 \text{ kcal/mol}$. The Wiener and London corrections increase the binding energy of two molecules by 10% each. If instead of the London correction we use the Kirkwood correction, the binding energy increases by an additional 20%. Comparison of the results of the Monte Carlo method with the real properties of water shows that, although the correlation corrections improve the agreement, a noticeable discrepancy remains, obviously associated with the nonpair intermolecular interactions. The correlation corrections reduce the equilibrium separation in a molecular dimer by 0.1 \text{ \AA}.

Sarkisov *et al.*^{22,23} developed a phenomenological interaction potential for water molecules, designed to reproduce the hydrogen bonds more accurately. The hydrogen bond potential in Refs. 22 and 23 is approximated by the Morse potential

$$u_{\text{OH}} = D \cdot \{1 - \exp(-a(r_{\text{OH}} - r_0))\}^2 - D \quad (5)$$

with parameters D , a , r_0 , adjusted to experimental data on

the stiffness and depth of the hydrogen bonds using results for the heat of sublimation of ice and the normal vibration frequencies in the water dimer. In Ref. 22 an attempt was made to refine the approximate formula (5) by replacing the parameter a with a functional dependence on separation according to

$$a(r_{\text{OH}}) = A_1 - A_2 \exp(-b(r_{\text{OH}} - r_0)^2). \quad (6)$$

However, the functional form (6) did not yield a noticeable change in the simulated properties of the liquid phase in comparison with $a = \text{const}$. The remaining interactions between molecular fragments, unrelated to the hydrogen bonds, are also localized at the atoms and are written in the 6-exp form suggested by Kitaigorodskii *et al.*,

$$u_{\text{HH}} = -(A/r_{\text{HH}})^6 + B \exp(-cr_{\text{HH}}) \quad (7)$$

and similarly for the O-O interaction.

Lemberg and Stillinger²⁴ did not treat the water molecules as rigid structures; instead, all three atoms of the molecule interact via central forces. The water molecule forms as a result of this interaction. In the process of dynamical growth of the system the molecules can be disrupted and then form again, and in the liquid phase the molecules can be replaced by protons. The most attractive feature of this approach is the systematic inclusion of non-pair contributions; all molecular deformation degrees of freedom are activated. The weak aspect of this approach is the need to introduce relatively stiff atom-atom potentials, entailing a small integration step for the particle equations of motion and consequently requiring a longer time to solve the equations. A similar problem also arises when this potential is used in the Monte Carlo method. The atomic interaction is written in the form

$$\begin{aligned} u_{\text{OH}}(r) &= \frac{A}{r^n} - \frac{2e^2}{r}, \\ u_{\text{HH}}(r) &= \frac{e^2}{r} + \frac{B}{1 + \exp(C(r-d))} \\ &\quad - D \exp(-E(r-f)^2), \\ u_{\text{OO}}(r) &= \frac{4e^2}{r} + \frac{F}{r^{12}} - \frac{G}{r^6}. \end{aligned} \quad (8)$$

The values of the parameters $A, B, C, D, E, F, G, d, f, n$ are determined so as to reproduce the normal vibration frequencies in the molecule and the binding energy in the molecular dimer. The results of simulations with this potential²⁵ are found to be in good quantitative agreement with the results of neutron-scattering experiments in water. Changes in the atom-atom potentials (8) introduced in Ref. 26 do not alter the basic idea of the approach. These corrections reduce the disagreement between the calculated internal energy and its experimental value in real water from 8 to 5%. Although improved agreement with experiment is also found in the value of the diffusion coefficient, it remains too small by approximately a factor of two. Much better agreement is found in the equilibrium microscopic properties according to diffraction data from

both x rays and neutrons. This relationship between the experimental results for real water and the equilibrium properties of the model proposed in Refs. 25 and 26 is probably explained by the fact that the atom-atom potentials (8) have been adjusted to yield a good description of the interaction near the energy minimum, whereas at the distances where the hydrogen bonds are disrupted these functions provide too crude a description. Judging by the diffusion coefficient, the interaction at intermediate distances is somewhat overestimated.

In the present work, as a result of analyzing the different potential models describing water molecule interactions, it is seen that the Rahman–Stillinger ST2 potential^{16–19} is preferable. The reasons for this conclusion are the following:

1. The good reproducibility of the microscopic properties of real water;
2. The effective incorporation of nonpair interactions in ST2;
3. The relative simplicity of the potential, as a result of which the arithmetic operations needed to calculate it are minimized;
4. The clear physical interpretation afforded by the potential;
5. The consistency of the water molecule based on ST2.

b) Water-ion interaction

The interaction between an ion and water molecules is characterized by the presence of strong electric fields which distort the charge distribution in the electron clouds of the molecule. Consequently, the nonpair contributions to the interaction energy are considerably stronger here. Despite this, the first treatments of water–ion system models attempted to effectively include the nonpair interactions in the pair potential. In using the molecular dynamics method to model water microclusters on ions, Briant and Burton⁷ represented the molecular structure of water in the same way as in the ST2 potential—four point charges in combination with a smoothing function and a source of the Lennard–Jones interaction localized at the oxygen atom. The ion was represented as a point source of the Coulomb field in combination with the Lennard–Jones interaction, expressed as a function of the distance between the ion center and the oxygen atom of a water molecule. A similar model was employed in Ref. 8. In Ref. 7 an iterative procedure was employed in which the parameters of the potential were varied in order to agree with the experimental values of the energy in ion–H₂O and ion–(H₂O)₄ clusters. A table of the resulting optimum parameters for the Lennard–Jones part of the potential, ϵ and σ , was given for Na⁺, Rb⁺, Cs⁺, F⁻, Br⁻, and I⁻. In Ref. 7 it was noted that this model is internally inconsistent due to the failure to include nonpair interactions. Thus, reducing the distance to the negative point charges in the water molecule model to 0.2 Å overestimates the binding energy in the Rb⁺(H₂O)₄ cluster while underestimating the values for F⁻(H₂O)₄.

The pair potential for the interaction between an ion and a water molecule, constructed using quantum-

mechanical calculations by the Hartree–Fock method, was employed in a Monte Carlo simulation of water microclusters on Li⁺, Na⁺, K⁺, Cl⁻, and F⁻ ions.^{9,27} Nonpair interactions were not taken into account. The Hartree–Fock potential was approximated by a distribution of point charges in the molecule, in combination with a short-range interaction between the charges and the ion center in the form of an exponential function of the distance between charges. Two models were used for the water molecule: with the charges in a single plane, and a more complicated three-dimensional distribution. The quantum-mechanical correlations of the electron densities were taken into account through corrections $\sim r^{-6}$ to the potential of Bernal and Fowler in the H₂O–H₂O interaction only. It was noted that in the ion–water molecular complexes the form of the H₂O–H₂O intermolecular potential is not critical, since the main role is played by the relatively strong interaction with the ions, and almost the same results are obtained with the ST2 potential.

The contributions from nonpair interactions in ion–water complexes were subjected to a thorough analysis in Ref. 10. The energy of the Li⁺–(H₂O)_{*n*} complexes (*n* = 1, 2, 3, 4) was calculated by the Hartree–Fock method in locally stable configurations, predicted in the approximation of a pairwise additive energy. The contributions from three-, four- and five-body interactions in a molecular cluster superposed on the Li⁺ electrostatic field were derived. Three-body interactions make up 3–10% of the energy, with the main contribution coming from triplets in which an ion takes part. Four-body interactions are weaker than three-body interactions by an order of magnitude. The overall conclusion is that the approximation using the assumption of pairwise additive interactions overestimates the binding energy in a cluster by about 10%. Even taking into account just three-body contributions yields a value for the binding energy which differs from the exact value by less than 1%.

A series of papers by Vogel *et al.*^{28–31} was published on molecular-dynamics modeling with periodic boundary conditions for water clusters of the electrolytes CsCl, NaCl, LiI, LiCl, CsCl, CsF at temperature 290–310 K. The ST2 potential was used to describe the H₂O–H₂O interaction and the interaction with the ions was modeled using point charges in combination with a Lennard–Jones potential. The radius σ and depth ϵ of the Lennard–Jones potential for different forms of water–water, cation–water, anion–water, cation–cation, anion–anion, and cation–anion interaction have different values. The water–ion potential has no smoothing function $s(r_{ij})$, but it is retained in the water–water interaction. Introducing $s(r_{ij})$ into the interaction with the ion leads to too abrupt a change in the slope of the potential curve between 4 and 5 Å and results in the formation of artificial “bubbles” in the liquid. The need to remove the spherically symmetric attenuation function from the ion–water potential is explained by the dominant role of the spherical part of the interaction in this case. The interaction here has no irregularities resulting from introducing two H₂O molecules interacting with the ST2 potential, displaced from the center of the point

charges, since the ion charge is guarded from such superpositions by the strong field of the repulsive part of the Lennard-Jones potential. In the absence of irregularity there is no need for the smoothing function $s(r_{ij})$.

Smoothing is introduced in the potential for the ion-ion interaction, but at large separations, not for small ones as in the case of the water molecules. The need for this smoothing arose from the cutoff of the ion interaction at large distances; the interaction is taken into account only with the ions in the individual periodic cell¹² and in the images in the 26 neighboring cells. The continuous decrease in the strength of the Coulomb potential at large distances is described in the functional form $\pm e^2(100 \cdot s(r) + 1)^{-1} r^{-1}$, where $s(r)$ is the Rahman-Stillingier smoothing function with spatial parameters $R_L = 9.3678 \text{ \AA}$, $R_U = 28.1034 \text{ \AA}$. The nonpair contribution to the energy of interaction with the ions are not taken into account explicitly. The atom-atom correlation functions, the energy distribution functions, and the self-diffusion coefficient were the main subjects of the analysis. Under strong electrolyte conditions CsCl (8 ions of Cs^+ and +8 ions of Cl^- in 200 H_2O molecules), the calculated self-diffusion coefficient was found to be too large by about a factor of 2.5 compared with the experimental value obtained by nuclear magnetic resonance for the same concentrations, but for a concentration four times as weak the agreement with experiment improved. The self-diffusion coefficient is found to be too sensitive to the correct formulation of the interaction at intermediate and large intermolecular separations, since the diffusive motion is accompanied by disruption and reestablishment of the intermolecular bonds. In constructing the model potentials the emphasis is primarily on the correct description of the region near the minimum potential. Consequently, the model potentials yield much more accurate results for liquid equilibrium microstructures and less reliable results for the transport coefficients.

The effective interaction potential between a water molecule and ions in a β -AgI crystal lattice was derived by Hale and Kiefer³² and applied in a numerical simulation by Ward *et al.*³³ The water molecule structure is given in the same way as in the ST2 potential, by four point charges with values of $\pm 0.2357e$ distributed at the vertices of a tetrahedron at distances of 1.0 \AA (positive) and 0.8 \AA (negative) from the center of the Lennard-Jones force. Nonpair interactions with ions were taken into account by introducing an isotropic polarizability $\alpha_w = 1.44 \text{ \AA}^3$ for the water molecule. The radius σ and depth ϵ of the Lennard-Jones potential are different in the interactions with Ag^+ and I^- : $\epsilon_{\text{Ag}^+} = 0.547 \text{ kcal/mol}$, $\epsilon_{\text{I}^-} = 0.622 \text{ kcal/mol}$, $\sigma_{\text{Ag}^+} = 3.17 \text{ \AA}$, and $\sigma_{\text{I}^-} = 3.34 \text{ \AA}$. The Ag^+ and I^- ions form a rigid geometrically perfect hexagonal β -AgI lattice with lattice parameters $a = 4.58 \text{ \AA}$ and $c = 7.494 \text{ \AA}$. Since the chemical bond between Ag and I is not purely covalent, the electron clouds included in the crystal structure of the Ag^+ and I^- ions partially overlap, which is responsible for an uncertainty in the charge localized at the ions. In Ref. 32 the value $Q = \pm 0.6e$ was determined, while in Ref. 33 it was $\pm 0.4e$. The value $\pm 0.6e$ was also used in earlier stud-

ies by different methods and different authors. The ion polarization in the electric field of the water molecule was also treated using the ion polarization coefficients $\alpha_{\text{Ag}} = 2.4 \text{ \AA}^3$ and $\alpha_{\text{I}} = 6.43 \text{ \AA}^3$. The variations in the polarization coefficients from their (ion) values to the atomic values for Ag and I give rise to variations in the binding energy of a water molecule with the AgI substrate by 6% (Ref. 32). The binding energy of a water molecule with lattice ions is described in the form

$$V(\mathbf{R}) = V_{LJ}(\mathbf{R}) + V_{el}(\mathbf{R}) + V_{ind}(\mathbf{R}), \quad (9)$$

where the Lennard-Jones potential accounts for the exchange and dispersive interactions,

$$V_{LJ}(\mathbf{R}) = \sum_{m=1}^M 4\epsilon_{mw} \left[\left(\frac{\sigma_{mw}}{|\mathbf{R}-\mathbf{r}_m|} \right)^{12} - \left(\frac{\sigma_{mw}}{|\mathbf{R}-\mathbf{r}_m|} \right)^6 \right], \quad (10)$$

the electrostatic part is

$$V_{el}(\mathbf{R}) = \sum_{i=1}^4 \sum_{m=1}^M \frac{q_i Q_m}{|\mathbf{r}_i - \mathbf{r}_m|}, \quad (11)$$

and the inductive part is

$$V_{ind}(\mathbf{R}) = -\frac{1}{2} \sum_{n=1}^M \sum_{m=1}^M \alpha_w \frac{Q_n Q_m (\mathbf{R}-\mathbf{r}_n) (\mathbf{R}-\mathbf{r}_m)}{|\mathbf{R}-\mathbf{r}_n|^3 |\mathbf{R}-\mathbf{r}_m|^3} - \frac{1}{2} \sum_{m=1}^M \sum_{i=1}^4 \sum_{j=1}^4 \alpha_m \frac{q_i q_j (\mathbf{r}_i - \mathbf{r}_m) (\mathbf{r}_j - \mathbf{r}_m)}{|\mathbf{r}_i - \mathbf{r}_m|^3 |\mathbf{r}_j - \mathbf{r}_m|^3}. \quad (12)$$

Here V_{ind} is a three-body interaction, where the first sum in Eq. (12) contains ion-water-ion interactions and the second contains water-ion-water interactions. The indices n and m run over all the ions, while i and j run over the labels of the four point charges in the water molecule centered at the point \mathbf{R} . Thus the Hamiltonian includes all third-order nonpair interactions, where triplets including an ion are treated explicitly and those not including an ion are treated implicitly in the ST2 potential. In the first sum of Eq. (12) for V_{ind} the off-diagonal ($n \neq m$) terms were neglected³² on the grounds that terms with $n \neq m$ have different signs depending on the relative orientation of $(\mathbf{R}-\mathbf{r}_n)$ and $(\mathbf{R}-\mathbf{r}_m)$, and so cancel out to a great extent. The contribution of the discarded terms is estimated to be 5%.

In the present work a model is developed for the interaction with ions proposed in Ref. 32, but with the difference that we retain all the terms in the first sum of Eq. (12). The need to discard off-diagonal terms arose in Ref. 32 on account of an unfortunate choice of notation: the sum contains too many (M^2) terms, which greatly increases the number of arithmetic operations required to evaluate the interaction at each step of the Monte Carlo procedure. The number of terms in the sum is reduced to M if we do not expand the quantities in parentheses in the original expression for V_{ind} :

$$V_{ind}(\mathbf{R}) = -\frac{1}{2} (\alpha_w \mathbf{E}_I(\mathbf{R}), \mathbf{E}_I(\mathbf{R}))$$

$$\begin{aligned}
& - \sum_{m=1}^M \frac{1}{2} (\alpha_m \mathbf{E}_w(\mathbf{r}_m), \mathbf{E}_w(\mathbf{r}_m)) \\
& = -\frac{1}{2} \alpha_w \left(\sum_{n=1}^M \frac{Q_n(\mathbf{R}-\mathbf{r}_n)}{|\mathbf{R}-\mathbf{r}_n|^3} \right)^2 \\
& \quad - \frac{1}{2} \sum_{n=1}^M \alpha_n \left(\sum_{i=1}^4 \frac{q_i(\mathbf{r}_i-\mathbf{r}_n)}{|\mathbf{r}_i-\mathbf{r}_n|^3} \right)^2;
\end{aligned}$$

$$\mathbf{E}(\mathbf{R}) = \mathbf{E}_I(\mathbf{R}) + \mathbf{E}_w(\mathbf{R}), \quad (13)$$

where $\mathbf{E}_I(\mathbf{R})$ is the electric field vector of all the ions at the point where the water molecule is located and $\mathbf{E}_w(\mathbf{r}_m)$ is the electric field vector of all the water molecules at the location of the m th ion. In expression (13) both sums contain up to M terms, but in the first of these the Cartesian components of the vector ($3M$ scalar terms) are summed, while in the second there are $12M$. In Ref. 32 the interaction between a single water molecule and the ions of the crystal substrate was studied, so that the Hamiltonian (12) has no water-ion-water terms involving *different* water molecules. In the present work we also disregard these off-diagonal terms in the energy. This approach implies that we are neglecting the interaction between the k th water molecule and the field of the electric dipole induced by the l th molecule on the ion with $k \neq l$. This type of interaction is weak because the electric field of the water molecule is much weaker than that of the ion. In addition, the signs alternate and the off-diagonal terms cancel in this interaction not only because of the randomness of the spatial positions of the water molecules with respect to the ion being polarized, but also the randomness of the relative orientations of the molecule. Since the error in the induced energy allowed in Ref. 32 was estimated to be 5%, in our more accurate model it must be at least a few times smaller.

After we discard the off-diagonal water-ion-water terms, the induced interactions in the system of K water molecules interacting with M ions of the crystal substrate is described in the form

$$\begin{aligned}
\sum_{k=1}^K V_{\text{ind}}(\mathbf{R}_k) & = -\frac{1}{2} \alpha_w \left(\sum_{n=1}^M \sum_{k=1}^K \frac{Q_n(\mathbf{R}_k-\mathbf{r}_n)}{|\mathbf{R}_k-\mathbf{r}_n|^3} \right)^2 \\
& \quad - \frac{1}{2} \sum_{n=1}^M \sum_{k=1}^K \alpha_n \left(\sum_{i=1}^4 \frac{q_i(\mathbf{r}_i^{(k)}-\mathbf{r}_n)}{|\mathbf{r}_i^{(k)}-\mathbf{r}_n|^3} \right)^2,
\end{aligned} \quad (14)$$

where k is the index of the water molecules. The importance of neglecting the off-diagonal nonpair water-ion-water interactions for the structure of expression (14) is that the number of terms containing R_k for each fixed index k is determined only by the number of ions M and is independent of the number of water molecules K . If we retain the off-diagonal terms in the sum (14), the number of terms grows to $M(K-1)$. In the Monte Carlo method at each step of the procedure used to realize the random Markov process, the change in energy due to the shift of a single molecule is calculated; for the Hamiltonian (14) this is M terms. In the general case, including off-diagonal

terms would necessitate the summation of $M(K-1)$ terms. Directly calculating such sums at each step would slow down the numerical implementation of the Markov process to such a degree that the calculations would be infeasible.

3. BOUNDARY CONDITIONS

The cluster approach in equilibrium statistical theory implies separating the phase space of the molecular system into regions. Each region is made to correspond with a subdivision of the system into relatively isolated molecular groups (clusters).^{11,34-37} In order to account for material, energetic, and mechanical contacts between a cluster and its environment we use an abbreviated statistical-mechanical description based on the idea of the Gibbs statistical ensemble. The energetic contact is described by the Gibbs canonical distribution function $\sim \exp(-H/kT)$, H with respect to the cluster microstage, where H is the energy and T is the temperature; the material contact is described by the distribution $\sim \exp(\mu N/kT)$ of the grand canonical ensemble, where N is the number of particles in a cluster and μ is the chemical potential; and the mechanical contact is described by the distribution in an isothermal-isobaric ensemble, $\sim \exp(-pV/kT)$, where V is the volume of the system and p is the pressure in the system; here μ , p , and T are specified as input parameters of the ensembles.

It is quite widely believed that the Gibbs equilibrium distribution is valid only in the thermodynamic limit where the number of particles satisfies $N \rightarrow \infty$; but the logic of the derivation of the Gibbs distribution^{38,39} shows that only two conditions are required for its validity: 1) the thermodynamic limit with respect to the number of particles in the heat bath with which the system in question is contact; 2) vanishingly small interaction between the system and the heat bath in comparison with the interaction energy inside the system. If the cluster satisfies these conditions, the principles of the Gibbs statistical mechanics can be applied to it regardless of the number of particles in the cluster.

Different statistical ensembles correspond to different boundary conditions. The microcanonical (NVH) ensemble corresponds to a completely isolated cluster; the canonical (NVT) ensemble corresponds to the presence of thermal contact only; the grand canonical ensemble (μVT) includes thermal and material contact; and the isothermal-isobaric ensemble (NpT) includes thermal and mechanical contacts with the macroscopic gaseous phase. The non-equivalence of the different ensembles for a system with a finite number of particles⁴⁰ is not a "defect" of the theory, but reflects the actual dependence of the thermodynamic behavior of a bounded molecular system on the specific boundary conditions.

A water cluster in the atmosphere is in contact with water vapor and the air medium. The saturation pressure p_a of the vapor is about three orders of magnitude smaller than the atmospheric pressure p_a , so that the mechanical contact between the cluster and the molecules of the gas phase itself can be neglected and we can take the pressure to be $p = p_a$. On the other hand, neglecting the solubility of

the air components in the water cluster implies that there is no material contact between the water nucleate and the other components, except for water vapor. Taking into account the low density of the water vapor $\rho \approx p_w/kT$ (the average separation between molecules is two orders of magnitude greater than the radius of the intermolecular interaction), we can calculate the chemical potential of the water molecules adequately using the ideal gas approximation

$$\mu = -kT \left\{ \frac{6}{2} \ln T + \ln \left[\frac{(2\pi mk)^{3/2} (2k)^{3/2} (J_1 J_2 J_3)^{1/2} 8\pi^{7/2} 8\pi^2}{gh^6} \right] - \ln \left(\frac{p_w}{kT} \right) \right\}, \quad (15)$$

where J_1, J_2, J_3 are the principal moments of inertia of a molecule and g is the molecular symmetry parameter (equal to 2 for H_2O). In the present work the cluster is assumed to be in material contact with the vapor with a chemical potential corresponding to the pressure p_w , and from (15) it is in mechanical contact with the air medium at a pressure p . It is in thermal equilibrium with both components at a temperature T . The calculation of the equilibrium thermodynamic properties reduces to a numerical average with respect to the equilibrium distribution functions over the cluster microstates. An exhaustive search of the cluster microstates (configuration) is carried out using a random Markov process realized with a computer. Successive stages involve displacement of the molecules, spatial rotation, introduction of new molecules, and removal from the system.¹²

In the first stage of the investigations the interaction between water clusters and individual ions is modeled. The strong electric field of a cluster produces a deep potential well for the water molecule whose spatial dimensions are smaller than the region bounded by the volume distribution function $\sim \exp(-pV/kT)$ and are on the order of the volume associated with a single molecule in the gas ($\sim kT/p$). Hence the weight factor $\exp(-pV/kT)$ has essentially no effect on the molecular distribution over cluster configurations; the walls of the cavity V are a long way from the cluster boundary. Physically this means that the mechanical contact with the air medium levels out in comparison with the strong interactions inside a cluster. Guided by this consideration, we replaced the volume distribution $\sim \exp(-pV/kT)$ with a fixed volume, i.e., we went over to a grand canonical ensemble with spherical boundary conditions. The volume of the spherical cavity containing the molecular motion is taken to be on the order of the volume per molecule in the atmosphere, $kT/p = 4 \cdot 10^3 \text{ \AA}^3$ ($T = 253 \text{ K}$, $p = 1 \text{ bar}$). Since the water vapor density in the atmosphere is two to three orders of magnitude less than the density of the atmosphere itself, the probability of finding a water vapor molecule not bound to a microdroplet in such a volume is close to zero; the ensemble-averaged number of molecules in this micro-

volume is treated as the cluster size, and this number remains essentially unchanged as V increases severalfold. The ion or ions that induce nucleation are located at the center of a spherical microcavity V of radius 10–20 Å. A cluster radius is usually less than 6–7 Å, so that there is essentially no mechanical contact with the walls; for larger clusters the size of the cavity should be increased by a factor of 1.5–2. A substantially larger cavity is undesirable, since in this case the probability that water vapor molecules are present in the system becomes larger. The algorithm does not allow for sorting of the molecules according to whether they are associated with the cluster or the gaseous phase, and such molecules are regarded as belonging to the cluster, which would somewhat increase its actual size. Random introduction and extraction of molecules from the microcavity is accounted for by the particle number distribution $\sim \exp(\mu N/kT)$, corresponding to material contact between the cluster and the water vapor.

4. ANALYSIS OF THE RESULTS OF THE NUMERICAL SIMULATIONS

According to the classical theory of capillarity,^{41–45} the nucleate of a dense phase in a gas is a uniform microscopic spherical structure. The free energy of such a nucleate consisting of N molecules can be estimated to lowest order as $G(N) = AN + BN^{2/3}$ ($A < 0, B > 0$). The first term represents contributions from “interior” particles and the second is the contribution from “surface” particles. The nonlinear dependence of $G(N)$ gives rise to a maximum in the work of formation of the nucleate, $A(N) = G(N) - \mu N$. The position $N = N_c$ of the maximum corresponds to the critical size of the nucleate. A critical nucleate is in unstable thermodynamic equilibrium with the gas and serves in a way as a barrier in the growth of a microdroplet. Large values of N_c for low vapor pressures correspond to a vanishingly small probability of spontaneous formation of critical nucleates, leading to metastable (recondensed) states of the gas. The penetration of extraneous nucleation centers (ions, crystalline microparticles, etc.) into the gas changes the behavior of $G(N)$. The path on which heterogeneous nucleation develops is determined by the specific form of the $G(N)$ profile of the nucleates that form in microimpurities. Two qualitatively different kinds of behavior are possible. In the first case the penetration of extraneous nucleation centers does not qualitatively change the profile $G(N)$; the curve remains convex and $A(N)$ has a maximum corresponding to the unstable critical nucleate, but the critical size of N_c is smaller than for homogeneous nucleation in a pure gas, i.e., nucleation starts at smaller values of the supersaturation. In the second case strong microscopic impurity fields qualitatively change the profile $G(N)$; the convex curve becomes concave and $A(N)$ acquires a minimum corresponding to the stable size of a microdroplet. Such stable microdroplets can take part in the nucleation process as independent particles, merging to produce larger objects. If the nucleation centers are ions the stable microdroplets that form are relatively large charged particles (clusters). When they merge these clus-

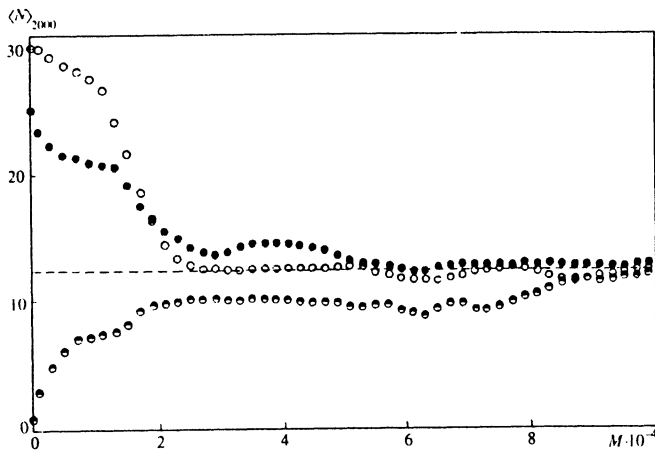


FIG. 2. The evolution in the number of water molecules in the field of an Ag^+ ion over 100,000 time steps on a variable section of the Markov process for $T=253$ K, $p=5$ mbar. The initial configuration was found through thermal equilibration of the system with a fixed number of particles over the course of 120,000 time steps. Here $\langle N \rangle_{2000}$ are partial averages over 2000 time steps; the broken trace is the average equilibrium number of molecules in the system over 600,000 successive time steps.

ters form drops of strong electrolytes. When nucleation follows this route it facilitates precipitation of salts, bases, and acid residues from the atmosphere.

Until recently it was assumed that the growth of water microdroplets on crystalline ions proceeds through the unstable critical dimension, i.e., $G(N)$ remains a convex function. On the basis of these ideas efforts have been concentrated on the calculation of the critical size. In Ref. 33 the critical size of a microdroplet on an AgI crystal substrate was estimated to be $N_c=3$ molecules. It is obvious that such a small value of N_c , if this turned out to be correct, could not retard nucleation, since the probability for the random formation of such a nucleate as a result of multiparticle molecular collisions is relatively large; fluctuations in the size in this case are comparable with the actual size of the nucleate. Hence the channels through which the nucleation process grows will develop with fluctuations that lie outside the bounds of successive addition of monomers to the microdroplet, as assumed in the standard kinetic theory. The very interpretation of the natural irregularities in the $G(N)$ profile for small values of N in Ref. 33 as a "critical size" raises doubts.

The results of the numerical simulations performed in the present work decisively imply that the electric field of an ion together with the exchange, dispersive, and polarization interactions stabilize the nucleate of a dense phase in H_2O vapor, i.e., the $G(N)$ curve changes qualitatively and becomes concave, while the work $A(N)$ has a minimum corresponding to the stable size $N=N_S$ of the nucleate. Calculations have been performed over a broad range of partial vapor pressures from $p=0.001$ mbar to 50 mbar at a temperature of 253 K. Spherically symmetric boundary conditions were employed; the system was placed in a spherical cavity of radius $R=10$ Å described about an Ag^+ or I^- ion center. The cavity bounds the system spatially, thereby restricting the growth of the gas phase around a seed with a given chemical potential. The average radius of a microdroplet is of order 5 Å, and a layer of the gas phase of approximately the same thickness separates the microdroplet from the walls of the cavity. Actually the microdroplet is in equilibrium with the gas, and the presence of the walls has almost no effect on the structure of the nucleate. The volume of the cavity is fixed (a μVT statistical ensemble applies), and all interactions between particles of the system are treated exactly.

One way to verify that a system in a numerical experiment is in thermodynamic equilibrium is the "control map" method.¹² A random Markov process, consisting of a succession of random attempts to move, augment, or diminish the particles in the system, is divided into a series of finite equal intervals with ΔM steps in each one. Partial averages are calculated on these intervals for the various statistical-mechanical properties of the system, and the dependence of these partial averages on the Markov "time" (the number of Markov steps taken) is analyzed. It can be shown⁴⁶ that when some natural requirements on the matrix of transition probabilities of the Markov process are satisfied, the behavior of the partial averages in Markov "time" qualitatively resembles the behavior of the corresponding quantities in real time and is determined by the profile $G(N)$. In a stable system the partial averages relax to their equilibrium values in the initial interval of the Markov trajectory and then fluctuate about these equilibrium values. This is precisely the behavior we observed for the number of water molecules attracted to the field of the ion in our numerical experiments. Figure 2 displays typical patterns for the change in the water molecule particle number in the field of an Ag^+ ion on the Markov trajectory. If the process begins with a number of molecules less than the stable size of a microdroplet, the microdroplet grows; in the opposite case it decreases to the stable size. It is well known that the stable existence of *macroscopic* phases in the μVT ensemble is impossible, since when the chemical potential μ varies continuously the density of the macrosystem changes discontinuously at the point of the phase transition. The electric field of the ion stabilizes the microdroplet, with the stable size of the nucleate being determined by the values of μ and T of the gaseous phase. In the present work each value of the partial vapor pressure was compared with the corresponding value of the chemical potential μ . This value of μ was substituted into the μVT ensemble distribution function in order to simulate the equilibrium between the microdroplet and the vapor. The use of the ideal-gas approximation for the vapor is justified, since the average separation between molecules at the pressures which were modeled was four orders of magnitude larger than the radius of the intermolecular interaction.

Figures 3 and 4 show radial density profiles in the microdroplet. At low pressures ($p < 1$ mbar) the first layer of water molecules forms at distances 2.9 Å (Ag^+) and 3.1

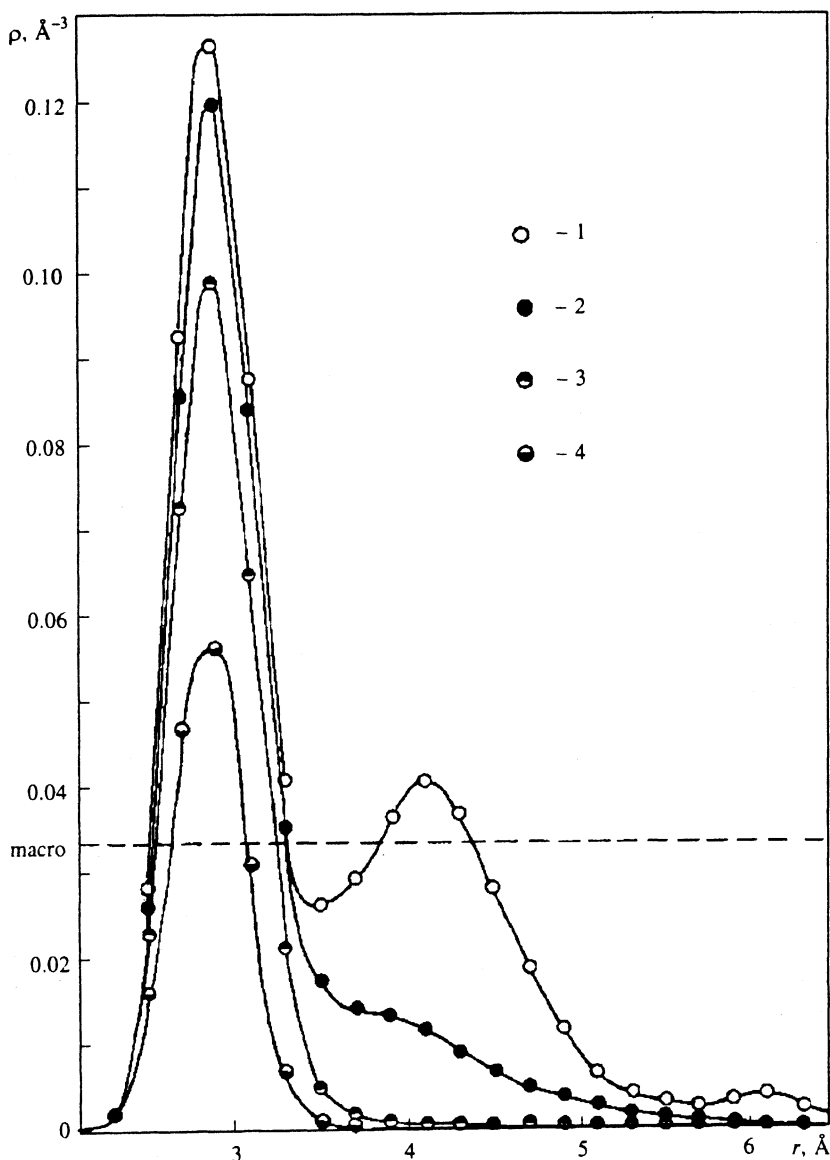


FIG. 3. The radial density distribution of the hydrated "jacket" around an Ag^+ ion at $T=253$ K; here r is the distance from the ion to the oxygen atom in the water molecule: 1) $p=50$ mbar; 2) $p=14$ mbar; 3) $p=1$ mbar; 4) $p=0.001$ mbar. The system is confined to the spherical cavity with radius $R=10$ Å. The broken trace represents the average total density in the macroscopic liquid phase under the same conditions.

Å (I^-) from the ion center; the layer thickness was 1 Å. As the pressure increases this layer becomes denser and reaches four times the average gross density in the macrosystem. In the pressure range $p > 1$ mbar a second layer of molecules begins to form. A second hydration lining forms at a distance of 4.1 Å from the ion center. At $p=50$ mbar a weak maximum is observed, corresponding to nucleation of the third hydration lining (Fig. 3). The separation between the first and second layers, 1 Å, is much less than the corresponding equilibrium separation in the $\text{H}_2\text{O}-\text{H}_2\text{O}$ molecular dimer, 2.9 Å, and approximately the same as the distance to the first maximum of the O-O binary correlation function in the macroscopic liquid phase.¹⁴ This implies that the water microstructure is severely distorted in the first two hydration layers. In fact, the equilibrium molecular structure exhibited in the macroscopic liquid phase is distorted by the strong electric field of the ion. The ion radius is 5% smaller than the I^- ion radius, and the first hydration layer on the Ag^+ ion is 20% more dense than in I^- . In the second hydration layer this difference flattens out.

The positive proton charges in the ST2 model are 1 Å from the geometrical center of the molecule, while the negative charges, which are displaced toward the oxygen atom, are at a distance 0.8 Å. The asymmetry of the charge distribution in the H_2O molecule gives rise to a selective interaction between the molecule and the positive and negative ions. After we average over the spatial orientation of the water molecule, other things being equal, the stronger interactions correspond to the negative ion; but the increase in the ion radius moves the interacting molecule away to greater distances and weakens the interaction. These two factors act in opposite directions. From a comparison of the distributions in Figs. 3 and 4 we see that the small ion radius of Ag^+ is the dominant factor in the first hydration layer. In the second hydration layer these two factors essentially cancel out.

The first coordination number can be found by integrating the first peak in the distribution. The uncertainty in its value stems from the strong dependence on the pressure of the vapor, with which the microdroplet is in equilibrium. From Figs. 3 and 4 we see that the concept of coord-

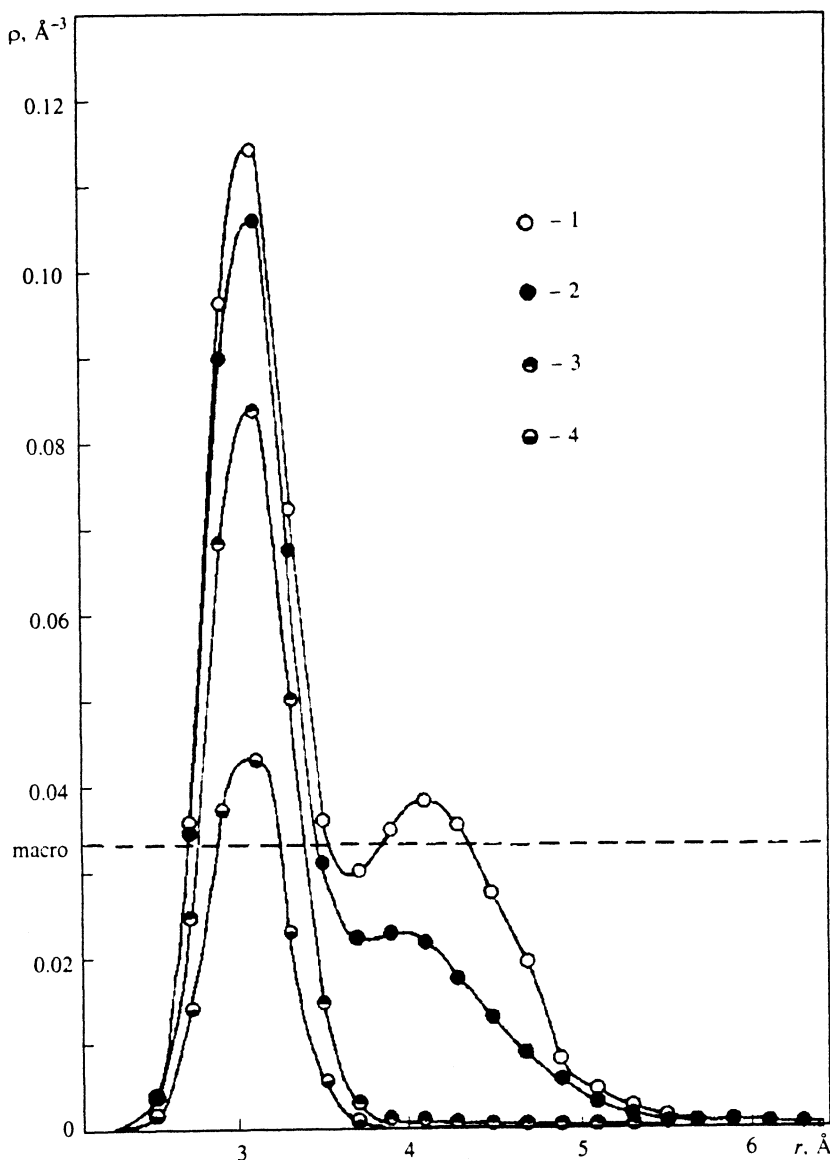


FIG. 4. As in Fig. 3, for I^- .

dination numbers for microcluster in a gaseous medium loses the precision associated with a microscopic liquid.

It is noteworthy that the equilibrium number of molecules precipitated on the ions remains greater than unity even when the moisture content in the surrounding gaseous medium is very low. Even for $p=10^{-4}$ mbar, which is several orders of magnitude below the saturation vapor pressure, each ion bears two water molecules on the average. This means that even under "dry" atmospheric conditions (in the usual sense) there are no free ions; each ion wears a hydration "jacket" of at least several H_2O molecules. The effective mass and radius of such an ion complex substantially exceed the mass and radius of a free ion. They determine the mobility and ultimately the diffusivity of the ions and the electrical conductivity of the atmosphere. This behavior becomes understandable if we take into account the substantial dipole moment and consequently the relatively strong interaction between the water molecule and the ions, which can reach 20–30 kT.

The layer-by-layer growth of a hydration "jacket" on

ions is manifested in the irregular variation of the stable size of a microdroplet as the vapor pressure increases. Figures 5 and 6 display the changes in the average number of water molecules trapped in the field of an ion as a function of the vapor pressure in the gaseous medium. The growth of the nucleate with increasing vapor density is reminiscent of the way electron shells in an atom fill up. The first hydration layer forms up to a pressure $p=10$ mbar; the increasing growth rate suggests an approach to a stable state with a completely filled shell. The subsequent growth for $p > 10$ mbar takes place due to accumulation of molecules in the second hydration layer. The initial formation stage of the second layer ($10 \text{ mbar} < p < 30 \text{ mbar}$) is retarded slightly: a "step" develops in the function $\langle N \rangle(p)$ (Figs. 5 and 6). For $p > 30$ mbar the growth rate on a logarithmic pressure scale increases by more than a factor of ten.

The free energy serves as a criterion for the strength of the binding between molecules and the cluster at finite temperatures. The direct calculation of free energy is a

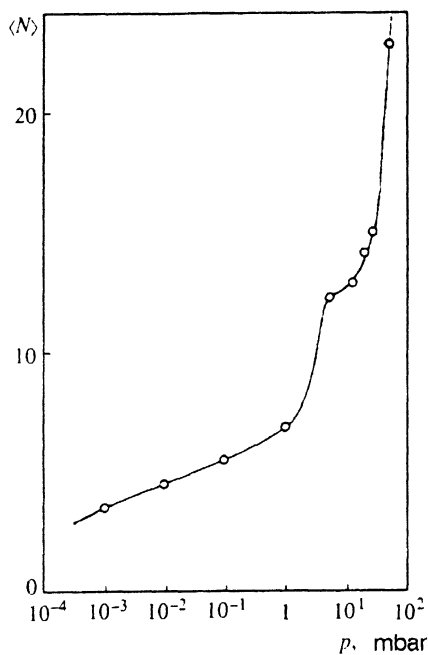


FIG. 5. The number of water molecules trapped in the field of an Ag^+ ion as a function of the vapor pressure in the gaseous medium at $T=253$ K.

problem in its own right and will be presented in forthcoming publications. The calculation of the internal energy in the numerical experiment is considerably simpler. Although the internal energy differs from the free energy by the entropy term, the behavior of the internal energy gives an idea of the mechanism for capture and retention of water molecules in a cluster. Figure 7 shows the average equilibrium interaction energy of particles in a microdroplet as a function of the microdroplet size $\langle N \rangle$.¹⁾ From the linear behavior of the total interaction energy of all the particles in the microdroplet we can conclude that the system has no well-defined internal stratified structure, but independent analysis of the energy of the interaction between the molecules and the ion and of the interaction energy of the molecules with one another argues the opposite. During the first stage of growth, up to $\langle N \rangle = 8$, the molecules in the microdroplets are confined only on account of their direct interactions with the ions; the average interaction energy of the molecules with one another is essentially zero. This stage corresponds to the "slow" growth of the microdroplet in Figs. 5 and 6 for $p < 1$ mbar. For $\langle N \rangle > 8$ the correlations between molecules become stronger, and the second mechanism for binding molecules to the microdroplet switches on, namely, the intermolecular interaction. The average intermolecular interaction energy, which is negative, increases in absolute value almost linearly, while the energy of the direct interaction with the ion grows more and more slowly (Fig. 7). This functional dependence shows that the accelerated growth of a microdroplet when a hydration layer is filling up is due not to the direct interaction with the ion but to the enhanced intermolecular correlations in the outermost hydration layer and the binding between molecules. This collective behav-

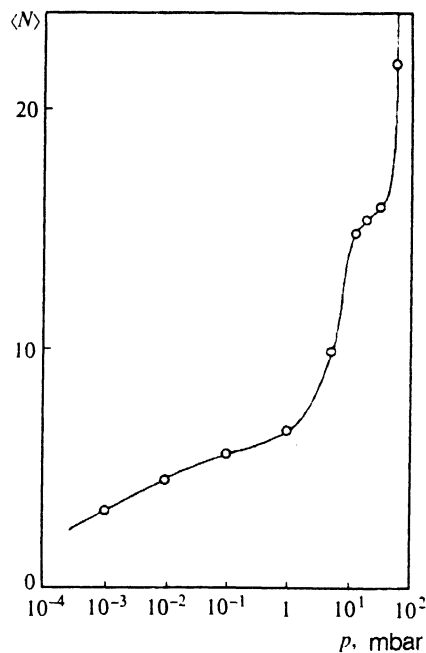


FIG. 6. As in Fig. 5, for I^- .

ior in the binding interactions will obviously become stronger as the distance from the ion increases, but even in the first hydration layer it is quite marked. From the functional behavior shown in Fig. 7 it is clear that in small microdroplets ($\langle N \rangle < 8$), collective effects appear somewhat weak when superposed on the strong electric field of the ion. Hence it is probably justified here to use the approximation in which we disregard the interaction of the water molecules with one another or an approximation in the spirit of the free-volume theory.

The abrupt qualitative change in the behavior of this system at $\langle N \rangle = 8$ is clearly seen in the dependence of $-\partial \langle U_{WW} \rangle / \partial \langle N \rangle$, which can be interpreted as the binding energy of a single molecule with the other molecules of the microdroplet (Fig. 8). We found this dependence by numerically differentiating the curve for $\langle U_{WW} \rangle$ in Fig. 7. It is clear that the binding energy with the water molecules increases almost discontinuously in absolute value from 0 to 0.3 eV (equal to $13.7 kT$). In contrast, the direct interaction with an ion sharply decreases from -0.5 eV ($= 22.9 kT$) to -0.2 eV ($9.2 kT$). It is evident that internal structural changes are taking place, and the molecular dipole moments are undergoing reorientation, leading to an enhancement in the interaction between them and a weakening of the direct interactions with the ions.

The results of the numerical simulation described in the present work can be summarized as follows.

1. The nucleates of the dense phase that form on the ions are thermodynamically stable.
2. The stable size of a nucleate under realistic conditions varies over a range from a few to 20–30 molecules, depending on the moisture content of the atmosphere.
3. The hydration "jacket" has a stratified structure, and the nucleate grows irregularly.

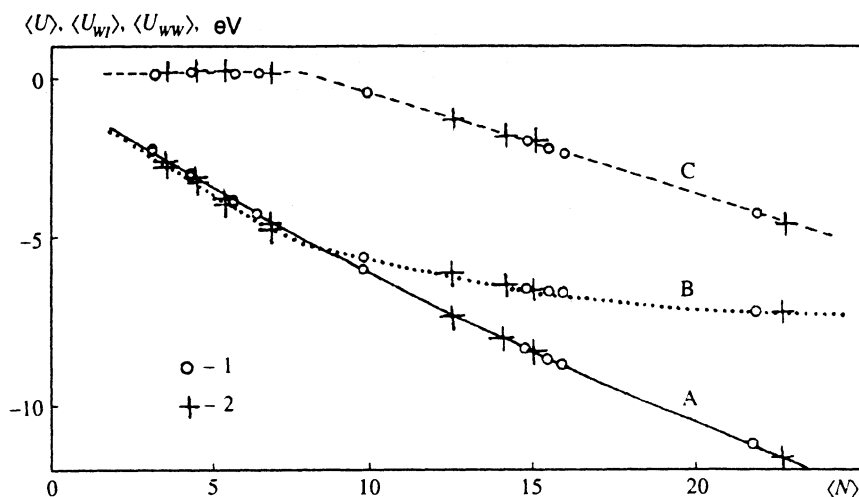


FIG. 7. The change in the microdroplet energy as a function of size: here $\langle U \rangle$ is the mean equilibrium interaction energy of all the particles in the system, $\langle U_{wI} \rangle$ is the interaction energy of all the water molecules with the ion, and $\langle U_{ww} \rangle$ is the interaction energy of the water molecules with one another: 1) microdroplet on an I^- ion; 2) microdroplet on an Ag^+ ion.

4. The molecules in the first layer are confined to the microdroplet due to their direct interactions with the ion. For $\langle N \rangle > 8$ the binding of molecules to the microdroplet changes qualitatively and becomes collective in nature.

5. Under realistic atmospheric conditions there exist essentially no free ions: all ions are hydrated. Their effective mass exceeds the mass of a free ion severalfold.

This work was available due to the financial support from the Russian Fund for the fundamental research. Project 93-05-8181.

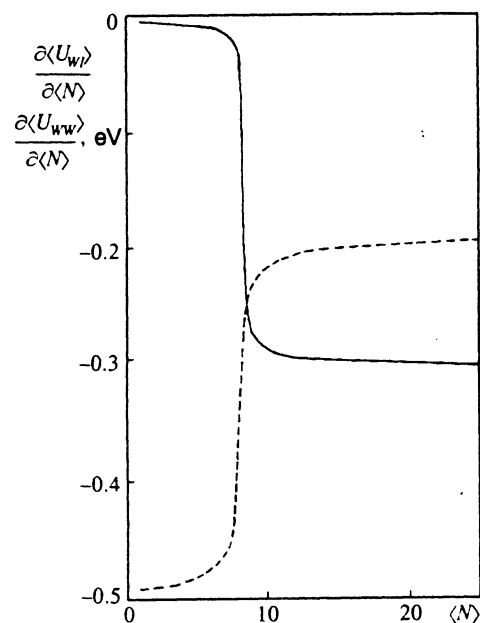


FIG. 8. Binding energy of a molecule in the microdroplet. Solid trace) interaction with the other water molecules in the water droplet; broken trace) interaction with the ion. The functions were found by numerical differentiation of the curves in Fig. 7.

¹⁾The internal energy of a microdroplet with a fixed center of mass differs from the average interaction energy by the trivial addition of the term $6/2\langle N \rangle kT$.

- ¹ C. L. Briant and J. J. Burton, *J. Chem. Phys.* **61**, 2849 (1974).
- ² C. L. Briant and J. J. Burton, *J. Chem. Phys.* **63**, 3327 (1975).
- ³ F. F. Abraham, *J. Chem. Phys.* **61**, 1221 (1974).
- ⁴ M. R. Mruzik, F. F. Abraham, D. E. Schreiber, and D. E. Pound, *J. Chem. Phys.* **64**, 481 (1976).
- ⁵ H. Popkie, H. Kistenmacher, and E. Clementi, *J. Chem. Phys.* **59**, 1325 (1973).
- ⁶ H. Kistenmacher, H. Popkie, and E. Clementi, *J. Chem. Phys.* **60**, 4455 (1974).
- ⁷ C. L. Briant and J. J. Burton, *J. Chem. Phys.* **61**, 2849 (1974).
- ⁸ C. L. Briant and J. J. Burton, *J. Chem. Phys.* **64**, 2888 (1976).
- ⁹ F. F. Abraham and M. R. Mruzik, *Faraday Disc. Chem. Soc.* **61**, 34 (1975).
- ¹⁰ H. Kistenmacher, H. Popkie, and E. Clementi, *J. Chem. Phys.* **61**, 799 (1974).
- ¹¹ T. L. Hill, *Statistical Mechanics. Principles and Selected Applications*, McGraw-Hill, New York (1956).
- ¹² V. M. Zamalin, G. E. Norman, and V. S. Filinov, *The Monte Carlo Method in Statistical Thermodynamics* [in Russian], Nauka, Moscow (1977).
- ¹³ J. A. Barker and R. O. Watts, *Chem. Phys. Lett.* **3**, 144 (1969).
- ¹⁴ A. Rahman and F. H. Stillinger, *J. Chem. Phys.* **55**, 3336 (1971).
- ¹⁵ F. H. Stillinger and A. Rahman, *J. Chem. Phys.* **57**, 1281 (1972).
- ¹⁶ F. H. Stillinger and A. Rahman, *J. Chem. Phys.* **60**, 1545 (1974).
- ¹⁷ A. Rahman and F. A. Stillinger, *J. Am. Chem. Soc.* **95**, 7943 (1973).
- ¹⁸ A. Rahman and F. H. Stillinger, *Phys. Rev. A* **10**, 368 (1974).
- ¹⁹ F. H. Stillinger and A. Rahman, *J. Chem. Phys.* **61**, 4973 (1974).
- ²⁰ F. H. Stillinger, *Adv. Chem. Phys.* **31**, 2 (1975).
- ²¹ R. O. Watts, *Mol. Phys.* **28**, 1069 (1974).
- ²² G. N. Sarkisov, V. G. Dashevsky, and G. G. Malenkov, *Mol. Phys.* **27**, 1249 (1974).
- ²³ V. G. Dashevsky and G. N. Sarkisov, *Mol. Phys.* **27**, 1271 (1974).
- ²⁴ H. L. Lemberg and F. H. Stillinger, *J. Chem. Phys.* **62**, 1677 (1975).
- ²⁵ A. Rahman, F. H. Stillinger, and H. L. Lemberg, *J. Chem. Phys.* **63**, 5223 (1975).
- ²⁶ F. H. Stillinger and A. Rahman, *J. Chem. Phys.* **68**, 666 (1978).
- ²⁷ M. R. Mruzik, F. F. Abraham, D. E. Schreiber, and D. E. Pound, *J. Chem. Phys.* **64**, 481 (1976).
- ²⁸ P. C. Vogel and K. Heinzinger, *Z. Naturforsch.* **30A**, 789 (1975).
- ²⁹ K. Heinzinger and P. C. Vogel, *Z. Naturforsch.* **31A**, 463 (1976).
- ³⁰ P. C. Vogel and K. Heinzinger, *Z. Naturforsch.* **31A**, 476 (1976).
- ³¹ K. Heinzinger, *Z. Naturforsch.* **31A**, 1073 (1976).
- ³² B. N. Hale and J. Kiefer, *J. Chem. Phys.* **73**, 923 (1980).
- ³³ R. C. Ward, B. N. Hale, and S. Terrazas, *J. Chem. Phys.* **78**, 420 (1983).

- ³⁴J. Frenkel, *J. Chem. Phys.* **7**, 200 (1939).
³⁵W. Band, *J. Chem. Phys.* **7**, 324 (1939).
³⁶W. Band, *J. Chem. Phys.* **7**, 927 (1939).
³⁷J. Frenkel, *J. Chem. Phys.* **7**, 538 (1939).
³⁸C. Kittel, *Introduction to Solid State Physics*, Wiley, New York (1956).
³⁹L. D. Landau and E. M. Lifshitz, *Statistical Physics*, Pergamon, Oxford (1980).
⁴⁰T. L. Hill, *Thermodynamics of Small Systems*, Vol. 1.2, New York-Amsterdam (1963).
⁴¹S. W. Thomson, *Proc. R. Soc. Edinburgh* **6**, 63 (1870).
⁴²R. V. Helmholtz, *Wiedemann: Ann. Phys. Chem.* **37**, 508 (1886).
⁴³J. W. Gibbs, *The Collected Works of J. W. Gibbs*, Vol. 1, Longmans, Green, New York (1878).
⁴⁴M. Volmer and A. Weber, *Z. Phys. Chem.* **119**, 277 (1926).
⁴⁵L. Farkas, *Z. Phys. Chem.* **A125**, 236 (1927).
⁴⁶S. V. Shevkunov, A. A. Martsinovskii, and P. N. Vorontsov-Vel'yaminov, *Teplofiz. Vys. Temp.* **26**, 246 (1988).

Translated by David L. Book